

# Free Energy Gap Dependence of the Electron-Transfer Rate from the Inverted to the Normal Region

N. Gayathri<sup>\*,†</sup> and B. Bagchi<sup>\*,†,‡,§</sup>

Solid State and Structural Chemistry Unit, Indian Institute of Science, Bangalore 560 012, India, and  
Department of Chemistry, University of Wisconsin, Madison, Wisconsin 53706

Received: April 26, 1999; In Final Form: August 12, 1999

A numerical study of the free energy gap (FEG) dependence of the electron-transfer rate in polar solvents is presented. This study is based on the generalized multidimensional hybrid model, which not only includes the solvent polarization and the molecular vibration modes, but also the biphasic polar response of the solvent. The free energy gap dependence is found to be sensitive to several factors, including the solvent relaxation rate, the electronic coupling between the surfaces, the frequency of the high-frequency quantum vibrational mode, and the magnitude of the solvent reorganization energy. It is shown that in some cases solvent relaxation can play an important role even in the Marcus normal regime. The minimal hybrid model involves a large number of parameters, giving rise to a diverse non-Marcus FEG behavior which is often determined collectively by these parameters. The model gives the linear free energy gap dependence of the logarithmic rate over a substantial range of FEG, spanning from the normal to the inverted regime. However, even for favorable values of the relevant parameters, a linear free energy gap dependence of the rate could be obtained only over a range of 5000–6000  $\text{cm}^{-1}$  (compared to the experimentally observed range of 10 000  $\text{cm}^{-1}$  reported by Benniston et al.). The present work suggests several extensions/generalizations of the hybrid model which might be necessary to fully understand the observed free energy gap dependence.

## 1. Introduction

A parabolic dependence of the logarithm of the electron-transfer rate on the free energy gap ( $\Delta G$ ) is, perhaps, the most dramatic prediction of the celebrated Marcus theory of electron transfer.<sup>1</sup> Many experimental studies have verified this bell-shaped prediction in charge-shift and charge-recombination reactions.<sup>2,3</sup> However, in contrast to the original Marcus prediction, the bell shape is often found to be asymmetric, the origin of which has been discussed extensively in the literature.<sup>4–6</sup> Many reasons have been put forth, including the involvement of the vibrational modes. In some ultrafast charge-recombination reactions, the contributions from the vibrational modes can be so strong as to lead to a marked deviation from the expected bell-shape dependence of the logarithmic rate.<sup>4,5</sup> Such deviations are referred to as the non-Marcus free energy gap (FEG) dependence of the rate. In many cases, the energy gap dependence has been found to be linear over a large energy gap, even on the order of 10 000  $\text{cm}^{-1}$ .<sup>5</sup> The reason for the validity of the exponential energy gap dependence of the rate over such a large variation of  $\Delta G$  is not clearly understood at present. In fact, this has remained one of the few long-standing unsolved problems in electron-transfer theory.

Substituent and isotope effects on the donor–acceptor pair within a charge-transfer system are known to significantly affect the free energy gap ( $\Delta G$ ) of the reaction.<sup>7</sup> Solvents also play a major role. Therefore, in experimental studies on the free energy gap dependence,<sup>4,5</sup> the electron-transfer reaction dynamics is observed in a series of donor–acceptor systems in a particular solvent. Interesting examples of non-Marcus free energy gap dependence have been found, with an off-parabolic behavior

pronounced, in some cases, in the normal region<sup>4</sup> and, in a few other cases, in the inverted region.<sup>8</sup> However, the nature of the non-Marcus FEG dependence can be quite different in these two, as discussed below.

**(i) Inverted Region.** In the famous Rehm and Weller experiments,<sup>8</sup> nonparabolic dependence with the rates higher in the inverted region than in the normal region was observed. Although it remained a paradox for a long time, this type of “breakdown” of the parabolic energy gap dependence has now been satisfactorily explained on the basis of the Collin–Kimball model.<sup>9</sup> The explanation is based on the Marcus theory itself, with a distribution of free energy values arising from the distribution of the distance between the donor–acceptor sites in a system. Such a broad distribution of free energy values essentially gives rise to contributions from many reactive pairs, some of which are present in the low-barrier region, leading to an enhancement of the rate. It is interesting to note that this effect is similar to that of the involvement of a high-frequency mode, as in the Jortner–Bixon model,<sup>10,11</sup> as both provide low barrier channels for the reaction to occur. We have discussed below the enhancement of the rate in the inverted regime via the Jortner–Bixon mechanism in more detail.

**(ii) Normal Region.** In the experiments of Asahi and Mataga,<sup>4</sup> the rates in contact ion pairs (CIPs) were found to be much higher in the normal region than in the inverted region and seemed to follow a near-linear dependence over the normal region.<sup>4</sup> On the other hand, in solvent-separated ion pairs (SSIPs), the rate was found to follow the Marcus parabolic dependence rather well.<sup>3</sup> An explanation such as that of the Collin–Kimball model is clearly not tenable for back ET in CIPs.

What then are the probable reasons for the observed non-Marcus dependence in the normal regime, such as in CIPs? A

<sup>†</sup> Indian Institute of Science.

<sup>‡</sup> University of Wisconsin.

<sup>§</sup> E-mail: bbagchi@sscu.iisc.ernet.in.

simple explanation using a 1-D description, with the reaction coordinate as the electrostatic potential difference ( $e\Delta V$  or  $X$ ) between the donor and the acceptor sites (which is produced by the surrounding polar solvent), was first put forward by Tachiya and Murata.<sup>12</sup> CIPs, like betaine-30, can be modeled as two-surface systems and are initially excited to a highly nonequilibrium state.<sup>13,14</sup> Therefore, the main assumption in the Marcus theory that the initial distribution of the system is at equilibrium may not hold for the CIP systems under study. Subsequent to the higher-level excitation, the CIP system relaxes toward the potential minimum of the excited surface. As a result, if the sink is in the normal region, there is a possibility for the system to react as it relaxes down. Of course, how much reaction takes place in this manner also depends on the electronic coupling strength  $V_{el}$  (or exchange integral  $J$ ) at the sink. When the value of the exchange integral is large (as is quite the case for the contact ion pairs), the reaction occurs with almost unit probability as the reactant population reaches the reaction zone. Thus, the reaction can occur from a completely nonequilibrium condition. On the other hand, when the value of  $J$  is small (as in the case for the solvent-separated ion pairs), only a small fraction reacts on the way to the potential minimum; the rest relax down toward the minimum of the excited surface, and further reaction occurs via the activated Marcus mechanism. Thus, in the case of small  $J$ , the reaction is always via the activated mechanism as the system has to relax after excitation, reach the potential minimum, and then overcome a reaction barrier.

Tachiya and Murata, restricting their description to a 1-D picture, showed that if one assumes a simple Smoluchowski dynamics for relaxation in a 1-D harmonic reactant potential surface and a  $\delta$  function sink for the reaction, then almost a quantitative explanation of the rate of charge transfer can be obtained for CIPs when  $J = 0.3$  eV and for SSIPs when  $J = 0.003$  eV. Tachiya and Murata had also reported the calculated energy gap dependence of the rate constant for various values of the exchange integral  $J$  in ref 12. In the case of  $J = 0.003$  eV, they found that the calculated energy gap dependence was essentially the same as that predicted from the Marcus theory.

However, although the model by Tachiya and Murata could explain the experimental results of Asahi and Mataga, the value of electronic coupling used for CIP was 0.3 eV, which is too large, and this is a point of serious concern, particularly if a nonadiabatic description is used. The reason that such a large value was required is that Tachiya and Murata assumed the entire reaction to occur from a single-point reaction site. As the electron transfer is required to occur during a single passage during the relaxation of the population toward the potential minimum, only a large  $J$  value can ensure a large probability of reaction. The scenario can change dramatically when broad reaction channels are present due to the presence or participation of vibrational modes.<sup>10,13–15</sup> In this work we demonstrate that this indeed happens and that one can explain the experimental results with much smaller coupling strength, on the order of 0.1 eV.

In the case of reactions in the inverted regime, such as in betaines, interplay between the solvent relaxation effects and the vibrational effects has been found to give rise to very large rates<sup>10,13,15</sup> as the presence of vibrational modes gives rise to additional reaction channels near the barrierless regions. In such systems, both experimental and theoretical observations clearly demonstrate the dominant role of vibrational modes.<sup>13–15</sup> There are several modes that are associated in an electron-transfer process such as the aromatic skeletal ring vibrations in aromatic

systems, torsional or bending motions, and intermolecular stretching modes. Also, exact identification of the nature of the vibrational modes that are involved is often difficult.<sup>7,24</sup> However, as first suggested by Barbara et al.,<sup>13,14,16</sup> the theoretical treatment of an electron-transfer process should be at least to a minimal level such as the hybrid model with one “average” low-frequency solvent mode, one average low-frequency vibrational mode, and one average high-frequency vibrational mode.

If the reaction is classically in the normal region, the presence of vibrational modes will only give rise to additional reaction channels in the higher normal region.<sup>19</sup> This means some of the sinks will be positioned closer to the excitation point (present in the normal region, as in CIPs), and so the rates may be larger. In addition, the presence of an ultrafast component, which is experimentally observed in nearly all the solvents, can enhance the rates.<sup>15,19</sup> The same interplay mechanism between solvent and vibrational effects, for a reaction involving nonequilibrium excitations such as in CIPs<sup>12,20</sup> and in betaines,<sup>13–15</sup> which was shown to be responsible for large rates in the inverted region, also holds good in the normal region. From the above discussions, it seems like the hybrid model can provide a unified description for the non-Marcus behavior in both the normal and the inverted regions.

Jortner and Bixon have earlier performed a detailed and elegant multimode, energy-dependent rate calculation<sup>17</sup> which could provide an explanation to the non-Marcus behavior. However, this description does not take into account the transient dynamics of motion on the potential energy surfaces as necessary to treat the scenario described in CIPs. A full dynamical calculation is required to understand the energy gap dependence, particularly when reactions can occur in the normal regime. It is in this regime, because of reaction possibilities in nonequilibrium conditions, that there is an interplay between the multi-time-scale relaxation effects of the reactant population after excitation and the differing charge-transfer strengths of the several broad sinks arising from the presence of the vibrational modes.<sup>15,18,19</sup>

One of the few unsolved problems in the theory of electron-transfer reaction is a quantitative explanation of the observed *linear* free energy gap dependence of the logarithm of the rate which has been experimentally observed over a large energy gap, covering in some cases even  $10\,000\text{ cm}^{-1}$ .<sup>4,5,17</sup> This spans the normal, barrierless, and inverted regimes. While it is clear that the elegant model of Jortner and Bixon in terms of the participation of many vibrational modes should form the backbone of any quantitative theory, several key factors still seem to be missing from this description. The following three appear to be particularly important.

(1) The effects of biphasic solvent relaxation on the electron-transfer rate. As these effect can be different from each other in the three (normal, barrierless, and inverted) regimes, this aspect needs further study.

(2) The hybrid model needs to be combined with the Collins–Kimbal<sup>9</sup> model of diffusion-limited ion pair recombination to describe experimental situations which involve electron transfer among ion pairs.

(3) It might be necessary to include the relaxation of the vibrational energy within the hybrid model. In the usual practice, electron transfer is assumed to occur from the *ground vibrational level* of the reactant to the excited vibrational states of the product surface. However, in photo-induced electron-transfer reactions, reactants are often produced in the vibrationally excited state. If vibrational energy relaxation is slow, then the

rate can be adversely affected. In particular, the initial part of the electron-transfer reaction (ETR) can be quite different. In fact, the initial part of the ETR can occur from the vibrational excited reactant states to the excited product states. The situation can be further complicated because of back electron transfer from the product to the reactant surface. In addition, back electron transfer from the product to the reactant surface needs to be considered if the electronic coupling is large.

Clearly each of the above three extensions is nontrivial. In the present paper, we have performed only the first one. We, however, present the tentative formulation for the other two cases. The main objective of the present study is to investigate the free energy gap dependence of the rate within the framework of the generalized hybrid model, with biphasic solvent response included. Also, in view of reported uncertainties in the estimation of the values of some of the solvent and vibrational parameters,<sup>17,28</sup> a detailed study of the dependence of the rate on a few relevant parameters was also carried out.

The results reveal a clear nonparabolic dependence of the logarithm of the rate on the free energy gap from the normal to the inverted regimes, spanning a range on the order of 5000–6000  $\text{cm}^{-1}$  in several cases of study. The results clearly indicate the wide range of possibilities that can arise within the framework of a minimal hybrid model. The analysis even with a simple one-dimensional Tachiya–Murata model revealed several interesting situations.<sup>20</sup>

The organization of the rest of the paper is as follows. In section 2, we describe the theoretical formulation of the hybrid model. In section 3 a dynamic version of the Tachiya–Murata model with the effects of vibrational modes in widening the sink is discussed. Section 4 includes a study of the dependence of the free energy gap dependence of the rate on various factors, such as solvent reorganization energy, solvent relaxation, and the frequency of the high-frequency mode. In section 5 we discuss the extensions of the present theoretical formulation required to treat experimental situations. Section 6 concludes with a brief discussion.

## 2. Theoretical Model and Formulation

As pointed out earlier, the effects of high-frequency vibrational modes are required to explain the high rate of the electron transfer as in betaine-30, which is in the “Marcus inverted region”.<sup>3–15,18,19</sup> In this case, the system is minimally modeled by a low-frequency, harmonic, and classical solvent mode ( $X$ ), a similar low-frequency vibrational mode ( $Q$ ), and a high-frequency, harmonic mode ( $q$ ). The high-frequency mode is treated quantum-mechanically. The potentials for the reactant and product states, therefore, become

$$V_{1n}(X, Q) = (1/2)2\lambda_X X^2 + (1/2)2\lambda_Q Q^2 + nh\nu_q \quad (1)$$

$$V_{2n}(X, Q) = (1/2)2\lambda_X (X - 1)^2 + (1/2)2\lambda_Q (Q - 1)^2 + nh\nu_q + \lambda_q + \Delta G \quad (2)$$

where  $V_{1n}$  and  $V_{2n}$  denote the reactant and product states, respectively, arising from the  $n$ th vibrational level of the high-frequency quantum mode.  $\Delta G$  is the free energy gap of the reaction.  $\lambda_X$ ,  $\lambda_Q$ , and  $\lambda_q$  are reorganization energies of the  $X$ ,  $Q$ , and  $q$  modes, respectively.  $\nu_q$  is the frequency of the quantum mode. A schematic representation of the hybrid model is shown in Figure 1. Since we are primarily interested in the photoelectron-transfer reactions, the reactant surfaces are often referred to as the locally excited (LE) states and the product surfaces as the charge-transfer (CT) states. In the hybrid model, therefore,

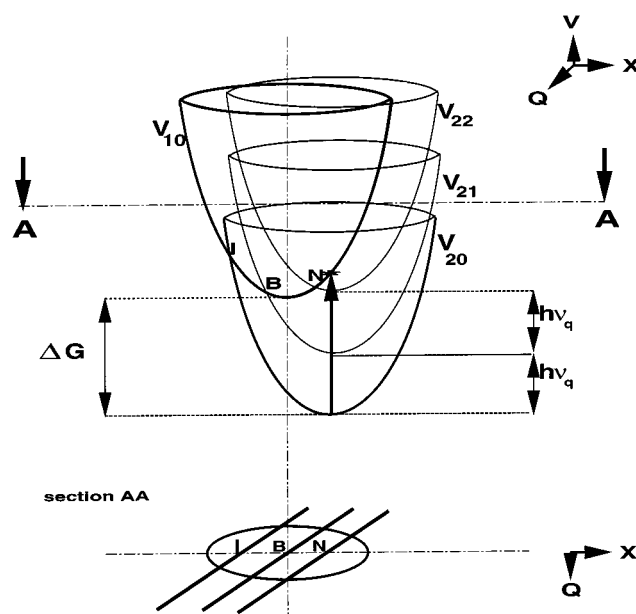


**Figure 1.** General multisurface schematic representation of the hybrid model for the electron-transfer reaction.  $V_{10}$  and  $V_{2n,n=0,1,2,\dots}$  are the effective potential energy surfaces for the ground reactant (or locally excited) states and the vibronic product (or charge-transfer) states, respectively.  $\Delta G$  is the difference between the potential heights between the ground reactant ( $V_{10}$ ) and the ground product ( $V_{20}$ ) states.  $h\nu_q$  is the quantum gap of the high-frequency vibrational mode. I, B, and N represent the inverted, barrierless, and normal cases, respectively. Section AA represents the projection of the harmonic potential surface  $V_{10}$  and the reaction (intersection) curves onto the  $X$ – $Q$  plane. The system is initially excited from the minimum of  $V_{20}$  surface to the  $V_{10}$  surface.

$\lambda_X$ ,  $\lambda_Q$ ,  $\lambda_q$ ,  $\nu_q$ ,  $\Delta G$ , and the electronic coupling strength  $V_{el}$  are the relevant parameters. However, the values of these parameters are often not known a priori. It is customary to obtain these values by fitting the experimentally obtained absorption intensity profiles to line-shape models.<sup>13,14,29</sup> The ETR reaction occurs only along the sink curves obtained by the intersections of the reactant and product potential energy surfaces (see Figure 1). The equations describing the sink curves can be obtained by equating eqs 1 and 2.

As the system is assumed to be excited from the ground charge-transfer surface ( $V_{20}$ ) onto the ground vibronic level of the locally-excited reactant surface ( $V_{10}$ ), the higher vibronic levels are not involved ( $V_{1n}$ ,  $n = 1, 2, \dots$ ) in the electron-transfer process. It is, therefore, sufficient to consider the electron-transfer reactive sites (sinks) that are present only along the intersections of the  $V_{10}$  surface with the product surfaces ( $V_{2n}$ ,  $n = 0, 1, 2, \dots$ ).

The quantum treatment of the high-frequency mode introduces a change in the effective free energy gap –  $\Delta G_n (= nh\nu_q + \lambda_q + \Delta G)$  between the ground reactant and  $n$ th product surfaces. One usually assumes that the relaxation of the high-frequency mode is much faster than any relevant process so the three-mode problem is reduced to a two-mode multisurface one. This approach can be easily generalized to an  $m$ -mode case where more than one high-frequency mode is involved. A subsection of the two-dimensional potential energy surface, cut horizontally at a height  $h$  on the  $V$ -axis and projected onto the  $X$ – $Q$  plane, would appear as an ellipse and the projected sink curves as parallel straight lines as in Figure 1. The ratio of the reorganization energies,  $\lambda_X/\lambda_Q$ , determines the effective sink width projected along  $X$ .<sup>11,19,21</sup> The sink reaction window is narrowed along  $X$  with increasing  $\lambda_X$ , and the dynamics is likely

to become more solvent controlled in such conditions, more so if the relaxation along the vibrational coordinate is much faster than that along the solvent coordinate.

A classical sink is said to be positioned in the normal region or in the inverted region depending upon whether  $\lambda$ , the sum of the reorganization energies  $\lambda_X$  and  $\lambda_Q$ , is greater than or lesser than  $-\Delta G_n$ , respectively. If the free energy gap  $-\Delta G_n > \lambda$ , then the classical Marcus picture predicts the electron-transfer reaction to be deeply in the inverted region and the reaction rate to be very small. When  $-\Delta G_n = \lambda$ , the barrierless case result, and when  $\Delta G_n < \lambda$ , a normal region case results.

In the presence of a high-frequency mode, multiple sinks are present. The projection of the sinks onto the  $X-Q$  plane would appear as shown in Figure 1, as already noted. However, the sinks are of differing strengths as the sink-transfer rate corresponding to the 0 to  $n$  transition involving the high-frequency mode is  $(2\pi V_{el}^2/\hbar)|\langle 0, n \rangle|^2$ , where  $V_{el}$  is the electronic coupling and  $|\langle 0, n \rangle|^2$  is the Franck-Condon overlap of the nuclear wave functions of the ground reactant and the  $n$ th product states. The Franck-Condon factor between the initial  $n^1$  state and the final  $n^2$  state is given by the relation

$$|\langle n^1, n^2 \rangle|^2 = \exp\left(-\frac{\delta^2}{2}\right) n^1! n^2! \left[ \sum_{r=0}^{\min(n^1, n^2)} \frac{(-1)^{n^1-r} (\delta^2/\sqrt{2})^{n^1+n^2-2r}}{r!(n^1-r)!(n^2-r)!} \right]^2 \quad (3)$$

where  $\delta^2 = 2\lambda_q/\hbar\nu_q$  is the coupling parameter. The rates can still be high in the inverted region because of the additional reaction channels opened up due to the high-frequency quantum levels; some of these channels may be not only efficient but also located near the barrierless region (or even in the normal region). But the main constraint is that the Franck-Condon overlap decreases rapidly with higher quantum levels of the CT states. As a result, most of the pertinent CT states that can contribute significantly to the transfer arise only from the lower quantum levels. For example, for the 0 to  $n$  transition, the maximum overlap is found for the (0, 2) or (0, 3) combination of levels in several cases as the  $\lambda_q$  is only around  $1000 \text{ cm}^{-1}$ . These have large energy gaps with respect to the LE state, and the transfer from the LE to CT state can, therefore, be assumed to be negligible. The inverted region case can then be treated as a single-surface ( $V_{10}$ ) problem with multiple sink windows. However, the above assumption may not be correct for an electron transfer in the normal regime especially when the sink reactive strength is large.

If the back transfer is neglected, then the time evolution of the probability distribution  $P_{10}(X, Q, t)$  of the system on the  $V_{10}$  PES is then given by the following equation:

$$\partial P_{10}(X, Q, t)/\partial t = (\mathcal{L}_X + \mathcal{L}_Q)P_{10}(X, Q, t) - S(X, Q)/P_{10}(X, Q, t) \quad (4)$$

The first term describes the relaxation in the  $V_{10}(X, Q)$  potential. The second term accounts for the actual transfer of the electron to the different CT states along the sink windows.  $\mathcal{L}_X$  and  $\mathcal{L}_Q$  are the Smoluchowski operators.  $S(X, Q)$  is the sink function. The latter is determined by both the energy considerations and the Franck-Condon overlap.<sup>15,19</sup> As already mentioned, the intrinsic sink-transfer rate ( $k_0$ ) corresponding to the 0 to  $n$  transition involving the high-frequency mode is  $(2\pi V_{el}^2/\hbar)|\langle 0, n \rangle|^2$ .

The operator  $\mathcal{L}_\xi$  ( $\xi = X, Q$ ) is assumed to be of the form

$$\mathcal{L}_\xi = D_\xi(t) \left( \frac{\partial^2}{\partial \xi^2} + \frac{1}{k_B T} \frac{\partial}{\partial \xi} \left[ \frac{dV(\xi)}{d\xi} \right] \right) \quad (5)$$

where  $D_\xi(t)$  is the time-dependent diffusion coefficient of motion along the reaction coordinate.  $D_\xi(t)$  is given by the relation<sup>23</sup>

$$D_\xi(t) = -k_B T d \ln \Delta_\xi(t) / dt \quad (6)$$

where  $\Delta_\xi(t)$  is the time correlation function of the  $\xi$ th reaction coordinate and is assumed to be of the form  $\sum_j w_j \exp(-t/\tau_j)$  where  $\sum_j w_j = 1$ . The diffusion coefficient is time-dependent when the relaxation is characterized by a multiexponential time decay (non-Markovian) and is time-independent only for a single-exponential decay (Markovian). The effective relaxation time  $\tau_{\text{eff}}$  is given by  $\int_0^\infty dt \Delta_\xi(t)$ . In the present treatment, the relaxation along the  $X$  mode has been assumed to be either overdamped Markovian or non-Markovian (biexponential) and that along  $Q$  mode to be infinitely fast (as in earlier theoretical studies).<sup>13,14,21</sup> Also, for simplicity, the initial population excited on the reactant (locally excited) surface may be characterized as a  $\delta$ -function source at  $(X_0, Q_0)$ . Mathematically, this is written as  $P_{10}(X, Q, t=0) = \delta(X-X_0) \delta(Q-Q_0) \delta_{1i}$ . In the case of back transfer reactions such as in CIPs,<sup>12-14,19</sup> the coordinates of the initial excited population correspond to those of the minimum of the ground (charge-transfer) surface (see Figure 1). The form of eq 2 implies that the minimum of the CT surfaces ( $V_{2n}$ ) are located at the coordinates (1, 1) on the  $X-Q$  plane.

The time-dependent solution of the dynamical equation (eq 5) describing the motion on a two-dimensional potential surface can be carried out by using Green's function technique.<sup>15,19</sup> The usefulness of this scheme lies in its generalization to the multidimensional potential energy surface and its ability to provide a solution even for the non-Markovian dynamics. Also, the formulation can be used to obtain the solution for a delocalized sink by employing a simple discretized form of any arbitrary delocalized sink function as a linear combination of  $\delta$  functions (for point sinks) with calculated weight factors.<sup>15,19,22</sup> Note that this discretization is perfectly general and valid for any delocalized sink and (or) an arbitrary initial distribution.

The time-dependent probability,  $P_{10}(t)$ , obtained using Green's function technique can be used to obtain the average rates of charge transfer. The average rate of the ET reaction ( $k_{\text{ET}}$ ) is defined as

$$\kappa_{\text{ET}}^{-1} = \int_0^\infty dt P_1(t) \quad (7)$$

However, when the solvation time correlation function is biphasic with widely different time scales, this method is not robust because evaluation of  $P_{10}(t)$  faces stability problems as this procedure is computationally intensive. Fortunately, there is a direct, almost analytical, method to obtain this average rate. This method uses the well-known Cramer technique to first obtain the solution of the system of linear equations by the matrix equation.<sup>15,19,22</sup> Also, this scheme is valid for any arbitrary sink.

### 3. Non-Marcus FEG Dependence of the Rate in the Normal Regime

To emphasize the need to extend the Tachiya-Murata model to a multidimensional description, we first present our investigations based on the Tachiya-Murata model.<sup>12</sup> The average rates obtained using a 1-D reaction picture (with only the solvation energy ( $X$ ) as the sole reaction coordinate), an initial Gaussian

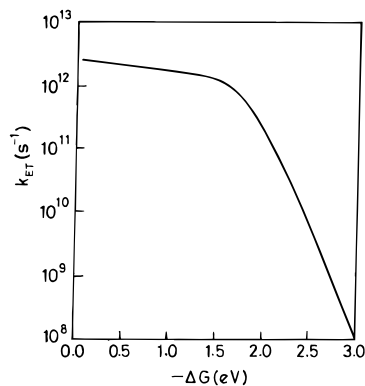


**Figure 2.** Average rate,  $k_{ET}$ , plotted as a function of the free energy change ( $-\Delta G$ ) showing the non-Marcus energy gap dependence for contact-ion pairs ( $J = 0.3$  eV). The small gap slow time decay component in  $P_1(t)$  may make  $k_{ET}$  dip near  $-\Delta G = 0$ . In this case,  $-\Delta G = 1.5$  eV is the zero-barrier point,  $-\Delta G < 1.5$  eV is the normal region, and  $-\Delta G > 1.5$  eV is the inverted region.

excitation distribution, and a  $\delta$  function point sink<sup>20</sup> are as shown in Figure 2, with the calculated average rate plotted against the free energy gap as in a standard Marcus plot. The rates were calculated using the parameter values as reported in Tachiya–Murata’s work: solvent reorganization energy ( $\lambda_X$ ) 1.5 eV, solvent relaxation time ( $\tau_X$ ) for acetonitrile 0.3 ps, and exchange integral (or electronic coupling  $V_{el}$ )  $J = 0.3$  eV. The results are found to be in good agreement with the experimental observations of Asahi and Mataga<sup>4</sup> when  $V_{el}$  is chosen to be 0.3 eV. The use of a broad initial (Boltzmann) distribution in this work in place of a  $\delta$  function distribution as in Tachiya and Murata’s work to describe an initial excited-state population on the locally excited surface (at the point corresponding to the minimum of the ground charge-transfer surface) did not result in any noticeable difference between the final rates obtained from these two works.

However, in the work of Tachiya and Murata, an unrealistically large value of the coupling strength ( $V_{el} = 0.3$  eV) was required to explain the results observed in CIPs. Usually, the values for  $V_{el}$  are obtained from the Hush approximation for the electronic coupling factors, and the reported values are most often in the range of 1400–2800  $\text{cm}^{-1}$  ( $\approx 0.11$ – $0.22$  eV).<sup>14,25</sup> Recently, uncertainties have been reported in the estimated values of the coupling strength,  $V_{el}$ .<sup>25,26</sup> Similarly, the solvent reorganization energy ( $\lambda_X$ ) values reported in the older literature span over a wide range ( $\approx 2000$ – $15000$   $\text{cm}^{-1}$ ). However, values on the order of 1–1.5 eV ( $\approx 7000$ – $15000$   $\text{cm}^{-1}$ ), such as used in the work related to the Tachiya–Murata model, are also suspected to be too high even in the case of strongly polar solvents, the error estimation being around 20%.<sup>26,28</sup> In some recent studies, the correction in  $\lambda_X$  has been more than 50%.<sup>28</sup>

In consideration of the above factors, we carried out investigations based on the hybrid model. In the presence of vibrational modes, several broad sinks are involved in the reaction, as explained earlier, and a large  $V_{el}$  value is not required. Thus, one may need to implement the hybrid model even in the normal region. The values of the parameters were chosen so that they are within the realistic limits<sup>13,14,29</sup> and are as follows: It is customary to obtain these relevant parameters

energy parameter	$\text{cm}^{-1}$	eV
solvent reorganization energy ( $\lambda_X$ )	2220	0.174
low-frequency mode reorganization energy ( $\lambda_Q$ )	1220	0.096
high-frequency mode reorganization energy ( $\lambda_q$ )	1228	0.097
quantum frequency ( $h\nu_q$ )	1550	0.122
electronic coupling strength ( $V_{el}$ )	1800	0.141

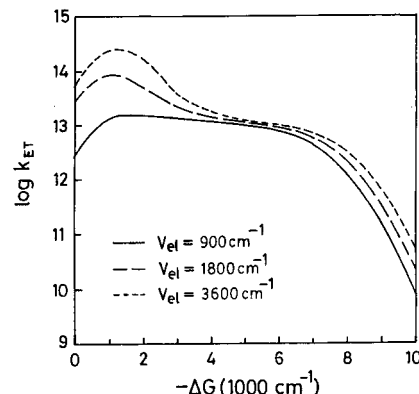


**Figure 3.** Sensitivity of the average ET rate ( $k_{ET}$ ) to the electronic coupling ( $V_{el}$ ) shown in the  $\ln k_{ET}$  vs  $-\Delta G$  plot for different values of  $V_{el}$ , 900, 1800, and 3600  $\text{cm}^{-1}$ .  $V_{el} = 900$   $\text{cm}^{-1}$  is much less than the value of 0.3 eV (3800  $\text{cm}^{-1}$ ) used in the Tachiya–Murata model. The results show nonlinearity in the high normal regime for larger  $V_{el}$  values. Values of the other energy parameters (in 1000  $\text{cm}^{-1}$ ):  $\lambda_Q = 1.5$ ,  $\lambda_q = 1.0$ , and  $h\nu_q = 1.8$ . The biexponential solvent time correlation function for acetonitrile is assumed to be  $\Delta(t) = 0.686 \exp(-t/0.089) + 0.314 \exp(-t/0.63)$ . Times are scaled in picoseconds.

by fitting the experimentally obtained absorption intensity profiles to line-shape models.<sup>13,14,29</sup> The above values are in good agreement with experimental results.<sup>15</sup> The values of some of the energy parameters were varied in various studies to gain an understanding of their effects on the ET rate. These results are presented in the following section.

Rate calculations were carried out using the method described in section 2 for three different values of  $V_{el}$  and by assuming a biexponential solvent relaxation for acetonitrile ( $\Delta_X(t) = 0.686 \exp(-t/0.089) + 0.314 \exp(-t/0.63)$ ) along the  $X$  mode and an infinitely fast relaxation along the  $Q$  mode. The results are shown in Figure 3. The rates were found to be rather large over much of the normal regime for all the cases and are clearly in contrast to the parabolic dependence. It is also clear from these results that the stronger the reactive sites and the closer they are to the excitation point, the faster is the rate. As pointed out earlier, the back transfer from the product to the reactant state could be substantial in the normal regime especially when the sink reactive strength is large and may give rise to lesser rates. However, efficient channels are located mostly near the barrierless region as the Franck–Condon overlap decreases rapidly with higher quantum levels of the CT states. For the parameters used, the maximum Franck–Condon overlap is usually found to be for  $(n, n + 2)$  or  $(n, n + 3)$  transitions.

For the case  $V_{el} = 900$   $\text{cm}^{-1}$  ( $\approx 0.07$  eV), the free energy gap dependence gives rise to an almost linear dependence above the barrierless region in the plot of  $\ln k_{ET}$  vs  $\Delta G$ . This behavior is very much similar to the one observed in CIPs. This demonstrates that the main limitations of the Tachiya–Murata model can be removed by use of the hybrid model. One can indeed explain the experimental observation with a realistic value of the coupling parameter by considering the effects from broad multiple sinks.

In the event of very low coupling strengths, it is intuitively obvious that the behavior would result in a bell-shaped Marcus dependence as seen in the case of charge recombination in weakly coupled SSIPs. So, perhaps, the hybrid model could provide a generic and realistic explanation to the non-Marcus behavior.

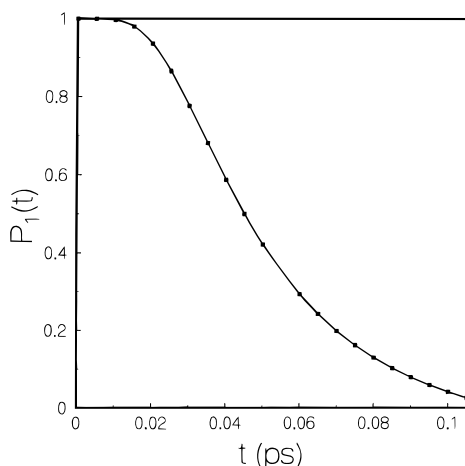


**Figure 4.** Time-dependent survival probability on the reactant surface,  $P_1(t)$ , plotted as a function of scaled time showing the nonexponential dynamics that are observed for the following set of values, deliberately chosen to mimic a normal region case. Values of the energy parameters (in  $1000 \text{ cm}^{-1}$ ):  $\lambda_X = 2.2$ ,  $\lambda_O = 1.5$ ,  $\lambda_q = 1.0$ ,  $\Delta G = 0.0$ ,  $\nu_q = 1.8$ , and  $V_{el} = 0.9$ . The biexponential solvent time correlation function for acetonitrile is assumed to be  $\Delta(t) = 0.686 \exp(-t/0.089) + 0.314 \exp(-t/0.63)$ . Times are scaled in picoseconds.

#### 4. Study of the Free Energy Gap Dependence of the Electron-Transfer Rate on the Solvent Relaxation Rate, Solvent Reorganization Energy, and Value of the Frequency of the Quantum Mode

Various reaction possibilities can be studied by varying the relevant solvent- and vibrational-related parameters in the hybrid model. As pointed out earlier, the values of some of these parameters are usually obtained from fits to experimental line-shape profiles<sup>13</sup> and are found to vary widely from system to system. However, as mentioned earlier, uncertainties in the estimation of these parameters, mainly  $V_{el}$ ,  $\lambda_X$ , and  $\nu_q$ , have been reported.<sup>25,26,28</sup> In view of this, we have carried out detailed studies to understand the sensitivity of the free energy gap dependence on these parameters. The results on the effects of electronic coupling,  $V_{el}$ , are already presented in the previous section. The other two studies related to  $\lambda_X$  and  $\nu_q$  are presented in this section.

As mentioned earlier, systems such as betaine-30 in a wide range of solvents have clearly revealed the interplay between the vibrational parameters and the ultrafast solvent relaxation components.<sup>15,18,19</sup> Only a limited number of vibrational channels are found to effectively participate in this enhancement as both the solvent relaxation rate and the intrinsic rate of the sinks compete to determine the choice of these sinks in the charge-transfer process. In acetonitrile, both the fast and slow time constants which characterize its biphasic relaxation ( $\Delta_X(t) = 0.686 \exp(-t/0.089) + 0.314 \exp(-t/0.63)$ ) behavior are in the sub-picosecond time scale. The slow relaxation effects (as those in alcohols) leading to very small ET rates are, therefore, not present in this case.<sup>18</sup>

An increase in the weight of the ultrafast component results in shifting of the average position of the relaxing population toward the potential minimum faster.<sup>15,18,19</sup> In such conditions, very fast and highly nonexponential reaction dynamics is possible in the normal region for systems initially excited to a highly nonequilibrium state as in betaines and CIPs. A time-dependent numerical study of the population reaction dynamics ( $P_1(t)$  vs  $t$ ) using a biexponential solvent relaxation for acetonitrile shows such very fast dynamics (Figure 4). As shown in our earlier work,<sup>20</sup> even a Markovian exponential relaxation shows highly nonexponential dynamics for the CIP case.

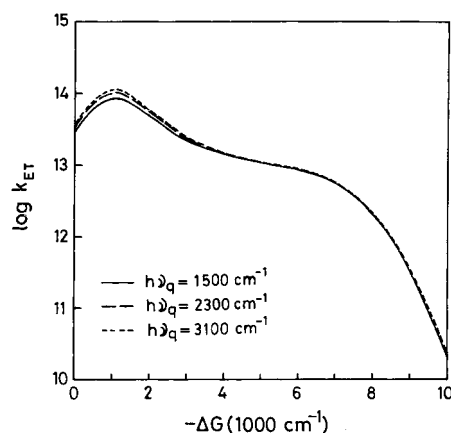


**Figure 5.** Sensitivity of the average ET rate ( $k_{ET}$ ) to the quantum frequency ( $\nu_q$ ) when the electronic coupling strength ( $V_{el}$ ) is  $2800 \text{ cm}^{-1}$  shown in the  $\ln k_{ET}$  vs  $-\Delta G$  plot for different values of the quantum frequency  $h\nu_q$ , 1500, 2100, and  $3100 \text{ cm}^{-1}$ . Values of the other energy parameters (in  $1000 \text{ cm}^{-1}$ ):  $\lambda_X = 2.2$ ,  $\lambda_O = 1.5$ , and  $\lambda_q = 1.0$ . The biexponential solvent time correlation function for acetonitrile is assumed to be  $\Delta(t) = 0.686 \exp(-t/0.089) + 0.314 \exp(-t/0.63)$ . Times are scaled in picoseconds. The rates are found to be not very sensitive to changes in  $h\nu_q$  as the reaction strengths of the sinks are quite strong due to a large  $V_{el}$  value.

Time-dependent studies involve rather extensive numerical computation and so have been restricted only to a single set of parameters. In the rest of the study, reaction rates were straightforwardly obtained.

The various results are presented in the following subsections.

**4.1. Effect of Change in the Frequency of the Quantum Vibrational Mode.** As demonstrated earlier in the case of betaines, the presence of a high-frequency mode can dramatically enhance the rate of electron transfer, particularly in the inverted region. It is easy to imagine that a range of reaction behavior is possible when only the quantum frequency is changed.

In fact, substituent and isotope effects on the donor–acceptor pair are known to significantly affect the frequency of the vibrational modes.<sup>7</sup> For example, the stretching frequency of the C–H bond decreases on deuteration. A reduction in the quantum frequency means more closely spaced sink channels involved in the reaction process. This does not immediately ensure an increase in the reaction rate because a major constraint is the rapidly decreasing Franck–Condon overlap value of the higher quantum levels of the product state. For this reason, when large energy gaps are involved, the rates are found to decrease on deuteration as the sinks close to the barrierless region become weaker.<sup>7</sup> Understandably, the charge-transfer rate is expected to be more sensitive to the changes in the high-frequency mode when the reaction is in the inverted regime.

We found that when sink strengths are quite large ( $V_{el} = 2800 \text{ cm}^{-1}$ ), the rates are rather insensitive to changes in the quantum frequency. This is shown in Figure 5. On the other hand, for a case study with a modest  $V_{el}$  value of  $1200 \text{ cm}^{-1}$ , the results are found to be otherwise as shown in Figure 6. The explanation is as follows. When the sink strengths are not very large, the overall rates are quite sensitive to the change in the density of the reaction channels, which occurs with a change in the frequency of the quantum mode. As mentioned earlier, there are many aspects which collectively determine the effectiveness of a sink, in particular the electronic coupling  $V_{el}$  and the solvent relaxation rates. While in Figure 5 above the results have been obtained with the biexponential relaxation data for acetonitrile ( $a_1 = 0.686$ ,  $\tau_1 = 0.089 \text{ ps}$ ,  $a_2 = 0.314$ ,  $\tau_2 = 0.63 \text{ ps}$ ), the results

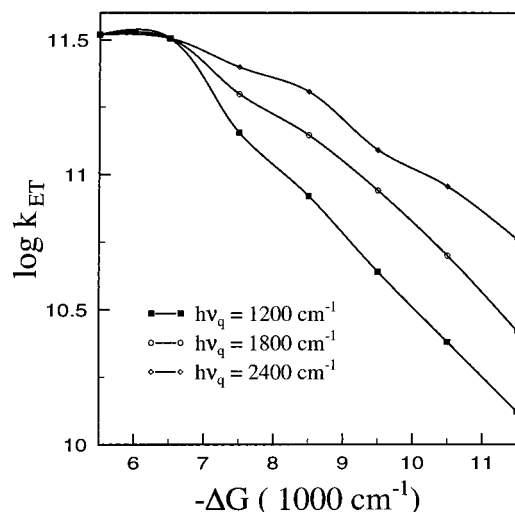


**Figure 6.** Sensitivity of the average ET rate ( $k_{ET}$ ) to the quantum frequency ( $\nu_q$ ) when the electronic coupling strength ( $V_{el}$ ) is  $1200 \text{ cm}^{-1}$  shown in the  $\ln k_{ET}$  vs  $-\Delta G$  plot for different values of the quantum frequency  $h\nu_q$ , 1200, 1800, and  $2400 \text{ cm}^{-1}$ . Values of the other energy parameters (in  $1000 \text{ cm}^{-1}$ ):  $\lambda_X = 2.2$ ,  $\lambda_Q = 1.5$ , and  $\lambda_q = 1.0$ . The biexponential solvent time correlation function for acetonitrile is assumed to be  $\Delta(t) = 0.65 \exp(-t/0.5) + 0.35 \exp(-t/20.0)$ . Times are scaled in picoseconds. The rates are found to be very sensitive to changes in  $h\nu_q$  as the reaction strengths of the sinks are not large due to a moderate  $V_{el}$  value.

of Figure 6 were obtained with slower relaxation time constants ( $a_1 = 0.65$ ,  $\tau_1 = 0.5 \text{ ps}$ ,  $a_2 = 0.35$ ,  $\tau_2 = 20 \text{ ps}$ ). The energy parameters are quite comparable between these two case studies. This shows that the *degree of the sensitivity of the free energy gap dependence to one particular parameter depends on other factors too.*

**4.2. Effect of Change in the Solvent Reorganization Energy.** The potential sensitivity of the rate to changes in the solvent reorganization energy ( $\lambda_X$ ) is obvious for the following reasons.

(1) Reorganization energies are the “force constants” in the quadratic equations (eqs 1 and 2) defining the harmonic potential energy surfaces and are highly important in determining the position of the classical sinks.

(2) The minimum activation energy ( $\Delta G_n^*$ ) of the reaction corresponding to the sink which arises from the  $n$ th vibronic product surface is also determined by the total reorganization energy ( $\lambda$ ) and is given by the relation<sup>11,15,21</sup>

$$\Delta G_n^* = (\lambda + \Delta G_n)^2 / 4\lambda \quad (8)$$

where  $\Delta G_n$  is the effective free energy gap for the  $0 \rightarrow n$  channel.

(3) The ratio of the reorganization energies,  $\lambda_X/\lambda_Q$ , determines the effective sink width, as mentioned earlier. The sink reaction window is narrowed along  $X$  with increasing  $\lambda_X$ , and the dynamics is likely to become more solvent controlled in such conditions.

Also, experimental studies have reported changes in  $\lambda_X$  with changes in solvent such as in the case of betaine in alcohols.<sup>29</sup> A study was, therefore, carried out to understand the sensitivity of the energy gap dependence to the solvent reorganization energy. The results are depicted in Figure 7 where  $\ln k_{ET}$  vs  $\Delta G$  behavior for three different values of  $\lambda_X$  is shown. The results clearly show the combined effects of the changes in the sink width and the activation energy with changes in  $\lambda_X$  over the whole range (of  $10 \text{ 000 cm}^{-1}$ ) of the free energy gap that

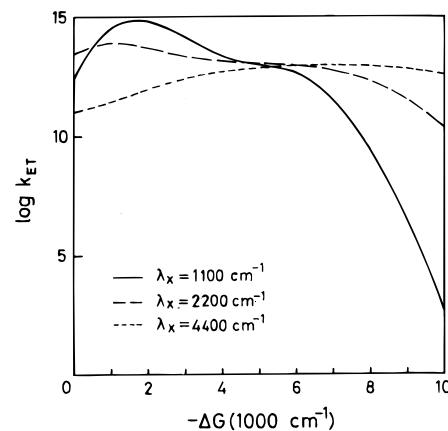


**Figure 7.** Sensitivity of the average ET rate to the solvent reorganization energy ( $\lambda_X$ ) shown in the  $\ln k_{ET}$  vs  $-\Delta G$  plot for different values of  $\lambda_X$ , 1100, 2200, and  $4400 \text{ cm}^{-1}$ . The biexponential solvent time correlation function for acetonitrile is assumed to be  $\Delta(t) = 0.686 \exp(-t/0.089) + 0.314 \exp(-t/0.63)$ . Times are scaled in picoseconds. The values of the other energy parameters (in  $1000 \text{ cm}^{-1}$ ):  $\lambda_Q = 1.5$ ,  $\lambda_q = 1.0$ ,  $h\nu_q = 1.8$ , and  $V_{el} = 2.8$ .

was studied. For the lower range values of  $\Delta G$  ( $\approx 5000 \text{ cm}^{-1}$  where  $\Delta G < \lambda$ ), most of the efficient sinks are likely to be present in the normal region. Also, as  $\lambda_X$  increases, the sinks are shifted to higher values of  $X$  with increases in  $\lambda_X$ . As these sinks in the normal region become closer to the excitation point, extremely high reaction strengths are required to trap the fast relaxing population. The rates were, therefore, found to decrease at a particular value of  $\Delta G$  with an increase in  $\lambda_X$ , reflecting the narrowing of the sink width and the shift of the sinks toward higher values of  $X$ . On the contrary, in the higher range values of  $\Delta G$  ( $\approx 5000 \text{ cm}^{-1}$  where  $\Delta G > \lambda$ ), an increase in  $\lambda_X$  shifts the sinks toward lower values of  $X$ . The rates were, therefore, found to increase in this region despite the narrowing sink width with increases in  $\lambda_X$  as most of the efficient sinks are likely to be shifted to the barrierless region.

Of course, the results shown here are for a single value of  $V_{el}$  equal to  $1800 \text{ cm}^{-1}$ . It is intuitively obvious that the sensitivity of the rate to changes in  $\lambda_X$  would also change with changes in the coupling strength. The effects of changing the coupling strength have already been discussed in section 3.

This study related to  $\lambda_X$  gains further relevance in view of several recent studies emphasizing the uncertainties in determining the value of  $\lambda_X$ , as mentioned earlier. A change in  $\lambda_X$  implies more changes—a shift in the position of the reaction site and its associated changes to activation energies and the effective sink widths. It is probable then that a system that was earlier perceived to be in the normal region could have as well been in the inverted region.

In view of the above, it is interesting to recall the argument of Asahi and Mataga,<sup>4</sup> who had argued that because of stronger charge-transfer complexation, the positions of the potential minima of the CIP state and the CT state remain close to each other; i.e., *the reorganization energy is likely to be small.* This makes the charge recombination (CR) in CIP to be in the inverted region for most of the values of  $\Delta G$ . However, the Asahi and Mataga argument that  $\Delta G$  must be much larger than the solvent reorganization energy would lead to rather small values of the rate for large  $\Delta G$ , at least in the classical picture, unless the interaction between the two surfaces is very large, which may again be unlikely even in the case of contact-ion pairs. This is because for small  $\lambda_X$  and large  $\Delta G$ , the classical crossing point in the Marcus 1-D reaction scenario would be

deeply in the inverted regime. For example, for  $\lambda_X = 2000 \text{ cm}^{-1}$  and  $\Delta G = -10\,000 \text{ cm}^{-1}$  (as in betaines), the classical crossing point along the  $X$  coordinate is at  $X_c = -8000 \text{ cm}^{-1}$  and the expected rate is on the order of  $10^{-6} \text{ ps}^{-1}$ , which is far too small.<sup>13,14</sup> However, as shown in several cases, the explanation of Asahi and Mataga can be resurrected by the presence of broader, multiple reactive sites arising from the vibrational modes that even the reactions that are classically in the inverted regime can proceed in the barrierless and (or) normal regimes.

## 5. Further Generalizations of the Hybrid Model

However, despite the demonstration of the non-Marcus behavior using the hybrid model and with a reasonably low value of  $V_{el}$  near linearity is observed only over a range on the order of  $5000\text{--}6000 \text{ cm}^{-1}$  or so (compared to the experimentally observed range of approximately  $10\,000 \text{ cm}^{-1}$  in CIPs) of the free energy gap spanning the normal, barrierless, and inverted regimes. In the very-deep-inverted regime, the rates are understandably smaller with reduced strengths of the sinks close to the activationless regime. It seems that a more comprehensive model could be obtained by combining the hybrid model with the Collin–Kimball model<sup>9</sup> (which was used to explain the non-Marcus behavior observed such as in the Rehm–Weller experiments<sup>8</sup>). Thus, the reactant probability distribution now depends not only on the solvent polarization coordinate  $X$  and the vibrational coordinate  $Q$ , but also on the separation distance  $R$  between the reactant pair. The dynamical equations for the hybrid Collin–Kimball model can be obtained by adding a diffusion term to the existing equation of motion and can be given in the following form:

$$\partial P_{10}(X, Q, R, t) / \partial t = (\mathcal{L}_X + \mathcal{L}_Q + \mathcal{L}_R) P_{10}(X, Q, R, t) - S(X, Q, R) P_{10}(X, Q, R, t) \quad (9)$$

$\mathcal{L}_R$  is the diffusion operator in real space to account for the migration of the reactant pairs. The sink function  $S(X, Q, R)$  is now determined not only by  $X$  and  $Q$ , but also by the distance of separation ( $R$ ) between the reactant pair. For different  $R$  values, the free energy gap is different for ion pairs.<sup>9b,c</sup> One thus would need to average over the initial distribution of  $R$ . The broad continuous sink area (*not a continuous line*) resulting in such a situation may render an extended linear behavior well into the inverted regime where reaction rates should increase. The operator  $\mathcal{L}_R$  is the diffusion operator with a mutual diffusion coefficient. Detailed numerical calculation with this model is yet to be carried out. There are, however, some qualitative conclusions which follow from the model. For all distances larger than the contact pair, the reorganization energy will increase, which in turn will enhance the distance-dependent Marcus rate of electron transfer between the reactant pair in the inverted region of FEG. The opposite will happen for the normal region. The overall effect can be significant.

In all the existing theoretical studies of electron-transfer reactions, relaxation of the high-frequency vibrational mode has been assumed to be infinitely fast. In many cases, this assumption is difficult to justify. Since reactants are often produced optically at highly vibrationally excited states, electron transfer can occur from these vibrationally excited states of the reactant to the vibrationally excited levels of the product state. We note here that the model presented here can be easily extended to accommodate such relaxation effects. The dynamical equations in such a case would be of the form

$$\partial P_{1n}(X, Q, t) / \partial t = (\mathcal{L}_X + \mathcal{L}_Q) P_{1n}(X, Q, t) - \sum_m S_{mn}(X, Q) P_{1n} \times (X, Q, t) + \sum_m S_{nm}(X, Q) P_{2m}(X, Q, t) - k_{1n} P_{1n}(X, Q, t) \quad (10)$$

where  $k_{1n}$  is the vibrational population relaxation rate of the reactant  $1n$  vibronic surface. A similar equation needs to be written for the population of the product  $P_{2m}$  states. The above master equation is general and includes the effects of the back reaction. There are two points of concern here. First, the rates  $k_{1n}$  can be small and rate determining. Second, the sink functions  $S_{nm}$  can peak at values different from those of the  $0 \rightarrow n$  channels involving the ground reactant surface  $V_{10}$ . Numerical studies indeed show that there are several efficient channels other than the  $0 \rightarrow n$  channel considered so far. This model can also be solved by extending Green's function method used in this study. One needs to consider an initial population distribution in the reactant, which can be in high nonequilibrium. This can seriously affect the rate of electron-transfer reactions.

Also, theoretical modeling, so far, involved only an average high-frequency mode to represent the overall contributions from the high-frequency factors.<sup>7,24</sup> Maybe, more than one high-frequency mode needs to be explicitly included in the parameter fitting of line shape profiles and in the formalism. This means more densely spaced sink channels. However, if the coupling strength is not very strong (as is the case in most systems), the product of Franck–Condon factors of the different high-frequency modes would tend to make the intrinsic rate from each sink small. The presence of several high-frequency modes may not, therefore, result in an increase of the ET rate.

It is to be noted that all the above suggested extensions to the model presented here can be solved using Green's function technique in a similar manner described in refs 15 and 19.

## 6. Conclusion

Let us first summarize the main results of this work. A detailed study of the free energy gap dependence of the rate of the electron-transfer reaction in a contact-ion pair in a polar solution has been carried out. The study is motivated by recent experimental and theoretical works which show distinct non-parabolic dependence of  $\ln k_{ET}$  vs  $\Delta G$ . A particularly interesting situation arises when the electron transfer is in the normal region of the free energy gap and when the value of the electronic coupling is reasonably large. The time dependence of the reactant population in such cases is predicted to be highly nonexponential.

It was expected that the minimal multidimensional model would suffice to explain the diverse behavior observed in ET reactions. A rather large number of parameters are involved even in a minimal model, and therefore, many different reaction scenarios are possible. The various results obtained from the investigation on the FEG dependence clearly indicate this. However, near linearity is observed only over a range on the order of  $5000\text{--}6000 \text{ cm}^{-1}$  or so (compared to the experimentally observed range of  $\approx 10\,000 \text{ cm}^{-1}$ ) of the free energy gap spanning the normal, barrierless, and inverted regimes in several cases. It seems, therefore, that a more comprehensive model could be obtained by combining the hybrid model with the Collin–Kimball model,<sup>9</sup> which was used to explain the non-Marcus behavior observed such as in the Rehm–Weller experiments.<sup>8</sup> This may render an extended linear behavior well into the inverted regime.

We have also pointed out that the assumption of an infinitely fast population relaxation along the vibronic states of the ground and excited surfaces may not be a valid one in certain cases.



Vibrational energy relaxations (VERs) of the high-frequency modes could be rather slow.<sup>30</sup> In such situations, two things need to be included: first, the possibility of electron transfer from the vibrationally excited states of the reactant and, second, the back transfer from the product to the reactant state (neglected in this study), particularly in the normal region. We have presented the model equation, which, however, has not been solved yet.

**Acknowledgment.** It is our pleasure to thank Professor Hans Heitele for his many valuable discussions. N.G. thanks the Council for Scientific and Industrial Research, India, for a Research Fellowship. This work was supported in part by the CSIR and DST (India) and the Theoretical Chemistry Institute, University of Wisconsin, Madison.

### References and Notes

- (1) Marcus, R. A. *J. Chem. Phys.* **1956**, *24*, 979. Marcus, R. A. *Annu. Rev. Phys. Chem.* **1964**, *15*, 155.
- (2) Miller, J. R.; Calcaterra, L. T.; Closs, G. L. *J. Am. Chem. Soc.* **1984**, *106*, 3047.
- (3) Mataga, N.; Asahi, T.; Kanda, Y.; Okada, T.; Kakitani, T. *Chem. Phys.* **1988**, *127*, 249.
- (4) Asahi, T.; Mataga, N. *J. Phys. Chem.* **1991**, *95*, 1961.
- (5) Benniston, A. C.; Harriman, A.; Philp, D.; Stoddart, J. F. *J. Am. Chem. Soc.* **1993**, *115*, 5298.
- (6) Nagasawa, Y.; Yartsev, A. P.; Tominaga, K.; Bisht, P. B.; Johnson, A. E.; Yoshihara, K. *J. Phys. Chem.* **1995**, *99*, 653.
- (7) Doolen, R.; Simon, J. D. *J. Am. Chem. Soc.* **1994**, *116*, 1155.
- (8) Rehm, D.; Weller, A. *Isr. J. Chem.* **1970**, *8*, 259.
- (9) (a) Collins, F. C.; Kimball, G. J. *Colloid Sci.* **1949**, *4*, 425. (b) Kakitani, T.; et al. In *Ultrafast Reaction Dynamics and Solvent Effects*; AIP Press: New York, 1993. (c) Murata, S.; Tachiya, M. *J. Phys. Chem.* **1996**, *100*, 4064.
- (10) Jortner, J.; Bixon, M. *J. Chem. Phys.* **1988**, *88*, 167.
- (11) Heitele, H. *Angew. Chem., Int. Ed. Engl.* **1993**, *32*, 359.
- (12) Tachiya, M.; Murata, S. *J. Am. Chem. Soc.* **1994**, *116*, 2424.
- (13) Walker, G. C.; Akesson, E.; Johnson, A. E.; Levinger, N. E.; Barbara, P. J. *J. Phys. Chem.* **1992**, *96*, 3728.
- (14) Akesson, E.; Johnson, A. E.; Levinger, N. E.; Walker, G. C. DuBruil, T. P.; Barbara, P. F. *J. Chem. Phys.* **1992**, *96*, 7859.
- (15) Gayathri, N.; Bagchi, B. *J. Phys. Chem.* **1996**, *100*, 3056.
- (16) Johnson, A. E.; Levinger, N. E.; Jarzeba, W.; Schleif, R. E.; Kliner, D. A. V.; Barbara, P. F. *Chem. Phys.* **1993**, *176*, 555.
- (17) (a) Cortes, J.; Heitele, H.; Jortner, J. *J. Phys. Chem.* **1994**, *98*, 2527. Bixon, M.; Jortner, J.; Cortes, J.; Heitele, H.; Michel-Beyerle, M. E. *J. Phys. Chem.* **1994**, *98*, 7289.
- (18) Gayathri, N.; Bagchi, B. *J. Chim. Phys.* **1996**, *93*, 1652.
- (19) Bagchi, B.; Gayathri, N. *Adv. Chem. Phys.* **1999**, *107 (II)*, 1.
- (20) Gayathri, N.; Bagchi, B. *J. Mol. Struct.* **1996**, *361*, 117.
- (21) Sumi, H.; Marcus, R. A. *J. Chem. Phys.* **1986**, *84*, 4272.
- (22) Samanta, A.; Ghosh, S. K. *Phys. Rev. E* **1993**, *47*, 4568.
- (23) Hynes, J. T. *J. Phys. Chem.* **1986**, *90*, 3701.
- (24) Dakhnovoski, Y. I.; Doolen, R.; Simon, J. D. *J. Chem. Phys.* **1994**, *101*, 6640.
- (25) Markel, F.; Ferris, N. S.; Gould, I. R.; Myers, A. B. *J. Am. Chem. Soc.* **1992**, *114*, 6208.
- (26) Bixon, M.; Jortner, J.; Verhoeven, J. W. *J. Am. Chem. Soc.* **1994**, *116*, 7349. Jortner, J.; Bixon, M. *Ber. Bunsen-Ges. Phys. Chem.* **1995**, *99*, 296. Jortner, J.; Bixon, M.; Wegewijs, B.; Verhoven, J. W.; Rettschnick, R. P. H. *Chem. Phys. Lett.* **1995**, *205*, 451. Jortner, J.; Bixon, M.; Heitele, H.; Michel-Beyerle, M. E. *Chem. Phys. Lett.* **1992**, *197*, 131. Jortner, J.; Bixon, M. *J. Photochem. Photobiol., A* **1994**, *82*, 5.
- (27) Bixon, M.; Jortner, J. *Chem. Phys.* **1993**, *176*, 467.
- (28) Karki, L.; Lu, H. P.; Hupp, J. T. *J. Phys. Chem.* **1996**, *100*, 15637.
- (29) Reid, P. J.; Barbara, P. F. *J. Phys. Chem.* **1995**, *99*, 17311.
- (30) (a) Oxtoby, D. W. *Adv. Chem. Phys.* **1979**, *40*, 1. (b) Oxtoby, D. W. *Annu. Rev. Phys. Chem.* **1981**, *32*, 77; *Adv. Chem. Phys.* **1981**, *47*, 487.